

Teaching antenna radiation from a time-domain perspective

Glenn S. Smith

School of Electrical and Computer Engineering, Georgia Institute of Technology, Atlanta, Georgia 30332-0250

(Received 29 March 2000; accepted 6 August 2000)

Radiation from a simple wire antenna, such as a dipole, is a topic discussed in many courses on electromagnetism. These discussions are almost always restricted to harmonic time dependence. A time-harmonic current distribution is assumed on the wire, and the time-harmonic radiated field is determined. The purpose of this paper is to show that simple wire antennas with a general excitation, e.g., a pulse in time, can be analyzed easily using approximations no worse than those used with time-harmonic excitation, viz. an assumed current distribution. Expressions are obtained for the electromagnetic field of the current that apply at any point in space (in the near zone as well as in the far zone). The analysis in the time domain provides physical understanding not readily available from the time-harmonic analysis. In addition, an interesting analogy can be drawn between the radiation from these antennas when excited by a short pulse of current and the radiation from a moving point charge.

© 2001 American Association of Physics Teachers.

[DOI: 10.1119/1.1320439]

I. INTRODUCTION

Electromagnetic radiation is a fundamental topic discussed in most undergraduate and graduate courses on electromagnetism. The basic formulas for radiation, that is, the integrals that give the potentials and field for a specified distribution of charge and current, are illustrated by application to some standard problems. Arguably, the most important of these is the radiation from a point charge moving along a prescribed trajectory. With reference to Fig. 1(a), at the observation point P , the electric field of the point charge q moving with velocity \mathbf{v} and acceleration \mathbf{a} is¹

$$\begin{aligned} \mathbf{E}(\mathbf{r}, t) &= \mathbf{E}_v + \mathbf{E}_a \\ &= \frac{q}{4\pi\epsilon_0} \left[\frac{(1-v^2/c^2)(\hat{\mathbf{R}}_q - \mathbf{v}/c)}{R_q^2(1-\hat{\mathbf{R}}_q \cdot \mathbf{v}/c)^3} \right]_{t_r} \\ &\quad + \frac{q}{4\pi\epsilon_0 c^2} \left\{ \frac{\hat{\mathbf{R}}_q \times [(\hat{\mathbf{R}}_q - \mathbf{v}/c) \times \mathbf{a}]}{R_q(1-\hat{\mathbf{R}}_q \cdot \mathbf{v}/c)^3} \right\}_{t_r}. \end{aligned} \quad (1)$$

where t_r is the retarded time

$$t_r = t - R_q(t_r)/c. \quad (2)$$

Here, the vectors \mathbf{r}_q and \mathbf{r} locate the charge and the observation point, respectively, and $\mathbf{R}_q = \mathbf{r} - \mathbf{r}_q$. The electric field in (1) is split into two components: the velocity field, \mathbf{E}_v , and the acceleration field, \mathbf{E}_a . The latter is proportional to the acceleration and accounts for the radiation from the charge, that is, for the portion of the field that falls off as $1/R_q$. From (1), it is clear that the temporal behavior of the radiated electric field depends directly on the temporal behavior of the velocity and acceleration at an earlier time (retarded time). The directional characteristics of the radiation field depend upon the relative orientation of the velocity and the acceleration. This is illustrated for two cases: *bremsstrahlung* in Fig. 1(b) where \mathbf{a} is parallel to \mathbf{v} , and *synchrotron radiation* in Fig. 1(c) where \mathbf{a} is perpendicular to \mathbf{v} . For both cases, the velocity is relativistic, $\beta = v/c = 0.9$. The radiation for the former is a narrow conical beam with a null in

the direction of the velocity, while the radiation for the latter is a narrow pencil beam with a maximum in the direction of the velocity.

A second problem often examined is the practically important one of radiation from thin-wire antennas. The discussion usually begins with a calculation of the radiation from the simple dipole or linear antenna shown in Fig. 2. In textbooks, the excitation for the antenna is taken, almost invariably, to be time harmonic with the angular frequency ω , and the distribution for the axial current along the arms of the antenna, each of length h , is assumed to be a standing wave:²

$$I(z, t) = \text{Re}[I(z)e^{j\omega t}], \quad (3)$$

where the phasor for the current is

$$I(z) = I_0 \frac{\sin[k_0(h-|z|)]}{\sin(k_0h)} U(h-|z|), \quad (4)$$

$k_0 = \omega/c = 2\pi/\lambda_0$, and U is the Heaviside unit-step function. The phasor for the radiated or far-zone electric field (the field in the limit as $k_0r \rightarrow \infty$) for this current is³

$$\mathbf{E}^r(\mathbf{r}) = \frac{j\mu_0 c I_0}{2\pi r} e^{-jk_0r} \left[\frac{\cos(k_0h \cos \theta) - \cos(k_0h)}{\sin(k_0h) \sin \theta} \right] \hat{\theta}. \quad (5)$$

For the special case of a dipole one-half wavelength long ($2h = \lambda_0/2$, or $k_0h = \pi/2$), the magnitude of this field is simply

$$|\mathbf{E}^r(\mathbf{r})| = \frac{\mu_0 c |I_0|}{2\pi r} \left| \frac{\cos[(\pi/2)\cos \theta]}{\sin \theta} \right|, \quad (6)$$

and the field pattern (a polar plot of $|\mathbf{E}^r|$ vs θ) is the familiar figure eight.

It is interesting to compare the two examples of electromagnetic radiation outlined above. For the moving point charge, the radiation at every point in space can be associated with the motion of the charge at a particular, earlier time. Thus, a physical understanding can be established that links characteristics of the radiation with elements of the motion. For the dipole antenna with time-harmonic excitation, the current essentially has existed on the antenna forever. The field at any point in space is a superposition of the fields due to the current at all points along the antenna; the

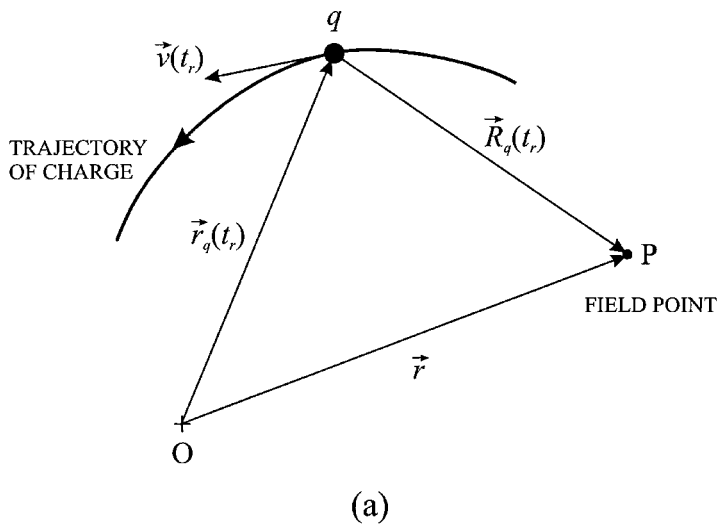
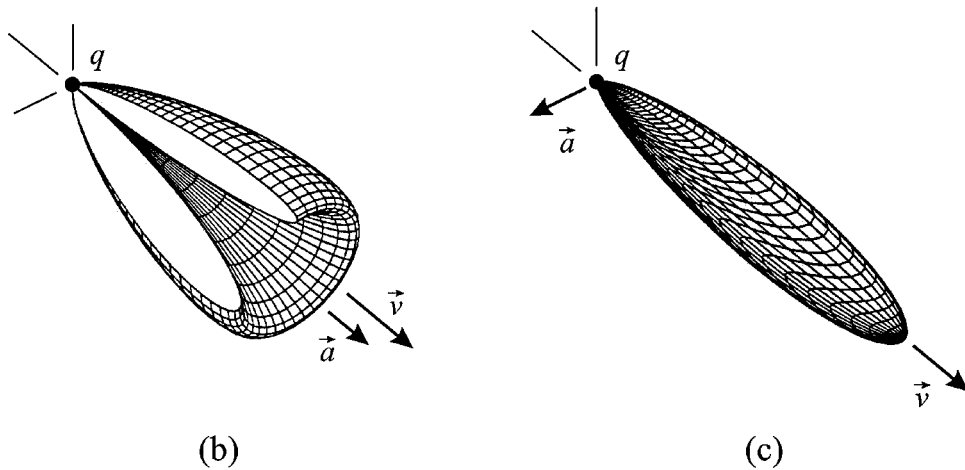


Fig. 1. (a) Trajectory for the moving point charge and the coordinates used in evaluating the electromagnetic field. Directional characteristics (power radiated per unit solid angle) for the radiation from the point charge when (b) the acceleration is parallel to the velocity, and (c) the acceleration is perpendicular to the velocity. $\beta = v/c = 0.9$.



current at each point, of course, is evaluated at a different earlier time. Thus, a one-to-one relationship cannot be established between characteristics of the radiation and the current at a particular point on the antenna. It would be instructive to

have a model for the antenna, similar to that for the moving point charge, that allows this correspondence.

In an earlier treatment, the author introduced the topic of radiation from wire antennas from a time-domain perspective—the current on the antenna was assumed to be a pulse in time.⁴ The radiated field of this current is no more difficult to obtain than for the current with harmonic time dependence; however, the physical understanding that can be obtained from this field is much greater. Several characteristics of the radiated field of the pulse-excited wire antenna are analogous to those for the radiated field of the moving point charge. Thus, this approach strengthens the physical understanding of electromagnetic radiation obtained when the two problems are treated in the same course. In the earlier treatment, only the radiated or far-zone field of the wire antenna was obtained. In this paper, the treatment is extended to include the field at all points in space. With this extension, the wave fronts near the antenna can be graphed and used to further the understanding of the process of radiation.

In Sec. II of the paper, we obtain exact expressions for the complete electromagnetic field (near field and far field) of an assumed, filamentary current distribution that we call the *basic traveling-wave element*. For illustrative purposes, the excitation for the element is chosen to be a Gaussian pulse of current/charge in time. In Sec. III, we show how the field of a wire antenna of general shape can be obtained as a superposition of the fields of a group of basic traveling-wave ele-

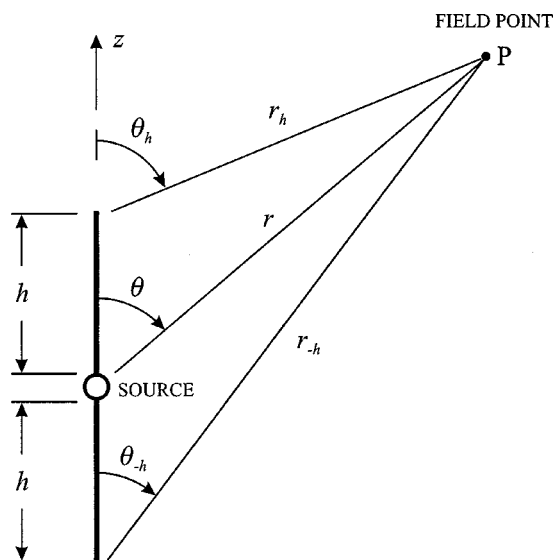


Fig. 2. Schematic drawing showing the standing-wave dipole antenna and the coordinates used in evaluating the electromagnetic field.

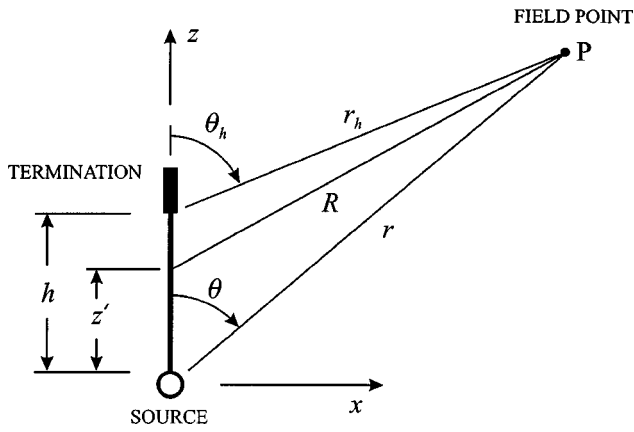


Fig. 3. Schematic drawing showing the basic traveling-wave element and the coordinates used in evaluating the electromagnetic field.

ments. In Secs. IV and V, this methodology is used to obtain the fields of a standing-wave dipole antenna and traveling-wave and standing-wave loop antennas. Throughout the paper, graphical results are used to illustrate the analogy between the radiation from these antennas when excited by a short pulse of current/charge and the radiation from a moving point charge.

II. THE BASIC TRAVELING-WAVE ELEMENT

To begin, we will introduce a structure that we call the basic traveling-wave element. This element is the building block out of which we will construct all other wire antennas. It can be thought of as an idealized model for a practical traveling-wave antenna.

The geometry for the basic traveling-wave element and the associated coordinates are shown in Fig. 3. The element of length h is aligned with the z axis. There is a source of current $I_s(t)$ at the bottom of the element and a perfect termination at the top of the element. We will assume that a traveling wave of current (a pulse) leaves the source and propagates along the element at the speed of light, c , until it reaches the termination, where it is totally absorbed. Thus the distribution for the axial current along the element is simply⁵

$$I(z,t) = I_s(t - z/c)[U(z) - U(z - h)], \quad (7)$$

and the charge per unit length on the element, as obtained in Appendix A, is

$$Q(z,t) = Q_s(t - z/c)[U(z) - U(z - h)] + q_0(t)\delta(z) + q_h(t)\delta(z - h), \quad (8)$$

where

$$Q_s(t) = I_s(t)/c, \quad q_0(t) = - \int_{t'=-\infty}^t I_s(t') dt', \quad (9)$$

$$q_h(t) = \int_{t'=-\infty}^t I_s(t' - h/c) dt',$$

and δ is the Dirac delta function. The three terms in (8) represent a traveling wave of positive charge, Q_s , propagating along the element at the speed of light, negative charge, q_0 , that is left behind at the lower end as the pulse of positive charge leaves the source (the element is always electrically neutral), and positive charge, q_h , that accumulates at the upper end as the pulse enters the termination.

The complete electromagnetic field of this current/charge is obtained in Appendix B:⁶

$$\mathbf{E}(\mathbf{r},t) = \frac{1}{4\pi\epsilon_0} \left[\frac{q_0(t-r/c)}{r^2} \hat{\mathbf{r}} + \frac{q_h(t-r_h/c)}{r_h^2} \hat{\mathbf{r}}_h + \frac{\cot(\theta/2)I_s(t-r/c)}{cr} \hat{\boldsymbol{\theta}} - \frac{\cot(\theta_h/2)I_s(t-h/c-r_h/c)}{cr_h} \hat{\boldsymbol{\theta}}_h \right], \quad (10)$$

$$\mathbf{B}(\mathbf{r},t) = \frac{\mu_0}{4\pi} \left[\frac{\cot(\theta/2)I_s(t-r/c)}{r} - \frac{\cot(\theta_h/2)I_s(t-h/c-r_h/c)}{r_h} \right] \hat{\boldsymbol{\phi}}. \quad (11)$$

Notice that two spherical coordinate systems are used in the description of this field; they are shown in Fig. 3: the system r, θ, φ with origin at the bottom of the element, and the system r_h, θ_h, φ_h with origin at the top of the element. The azimuthal coordinate is the same in both systems, so $\hat{\boldsymbol{\phi}}_h = \hat{\boldsymbol{\phi}}$.

In the limit as $r \rightarrow \infty$, or more precisely as $r/c\tau \rightarrow \infty$ where τ is a characteristic time associated with the duration of the current, (10) and (11) simplify to become the radiated or far-zone field of the element:

$$\mathbf{E}'(\mathbf{r},t) = \frac{\mu_0 c \sin \theta}{4\pi r (1 - \cos \theta)} \{ I_s(t - r/c) - I_s[t - r/c - (h/c)(1 - \cos \theta)] \} \hat{\boldsymbol{\theta}}, \quad (12)$$

$$\mathbf{B}'(\mathbf{r},t) = \frac{1}{c} \hat{\mathbf{r}} \times \mathbf{E}'(\mathbf{r},t). \quad (13)$$

In the examples that follow, the current of the source in (7) is assumed to be a Gaussian pulse of the form

$$I_s(t) = I_0 e^{-(t/\tau)^2}, \quad (14)$$

where τ is the characteristic time. The time for light to travel the length of the element is $\tau_a = h/c$. In the examples, we will choose $\tau/\tau_a = 0.076$; then, the width of the pulse in space is approximately one-fourth of the length of the element (four pulses fit along the element).

Figure 4 shows the electric field surrounding the traveling-wave element at three times: $t/\tau_a = 0.5, 1.5,$ and 2.5 . Here, the logarithm of the magnitude of the electric field, $|\mathbf{E}|$, is plotted on a gray scale, and the range for the values of $|\mathbf{E}|$ displayed is 100:1.⁷ The pulse of current/charge travels up the element until it reaches the termination where it is absorbed. In Fig. 4(a), the pulse is halfway up the element, and in Figs. 4(b) and 4(c), the pulse has been absorbed by the termination. A spherical wave front W_1 , centered at $z=0$, is produced when the pulse leaves the source, and a second spherical wave front W_2 , centered at $z=h$, is produced when the pulse is absorbed by the termination. These wave fronts travel outward from the ends of the element at the speed of light. Notice in Fig. 4(c) that there are strong electric fields about the source and the termination not associated with these wave fronts. The traveling-wave element is elec-

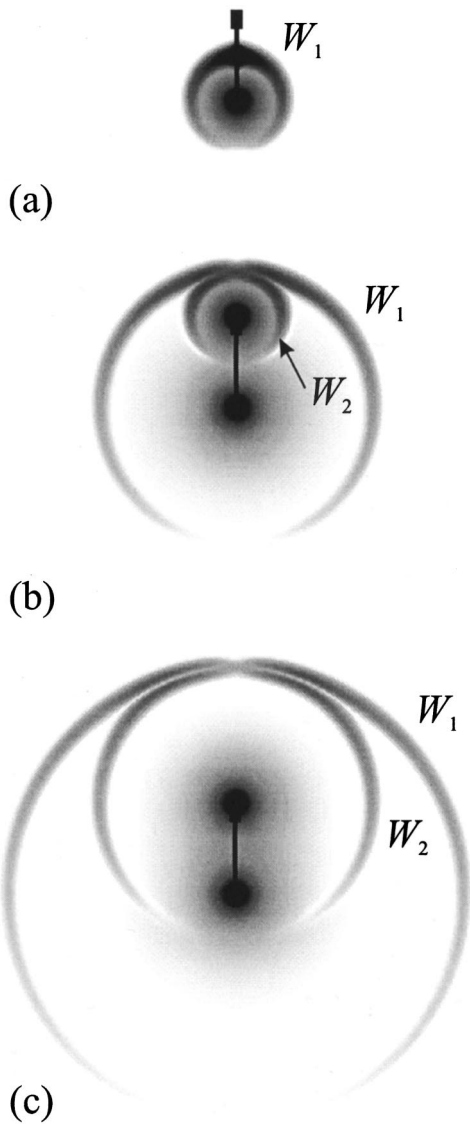


Fig. 4. The magnitude of the electric field surrounding the basic traveling-wave element at three times: (a) $t/\tau_a=0.5$, (b) $t/\tau_a=1.5$, and (c) $t/\tau_a=2.5$. The excitation is a Gaussian pulse with $\tau/\tau_a=0.076$.

trically neutral, so negative charge remains at the source after the pulse of positive charge leaves, and positive charge accumulates at the termination as the pulse arrives. These charges produce static electric fields about the two ends of the element.

Figure 5(a) is a drawing detailing the scheme we will use for plotting the radiated or far-zone electric field. A spherical surface of large radius, r , is centered at the source. Observers are stationed at points equally spaced in the angle θ on this sphere, e.g., at the angles $\theta=0^\circ, 22.5^\circ, 45^\circ, \dots$. Each of the observers records the radiated electric field at their position as a function of the normalized time t/τ_a , where t is now the time with the common delay r/c removed. Figure 5(b) shows the plots made by these observers. The time axis for each plot points in the direction of the observer, and the times $t/\tau_a=0$ for all of the plots lie on a circle.⁸ A dashed line in Fig. 5(b) connects the times of arrival associated with each of the two spherical wave fronts, W_1 and W_2 , shown in Fig. 4.

At any angle shown in Fig. 5(b), there are two Gaussian pulses of electric field, one associated with each wave front.

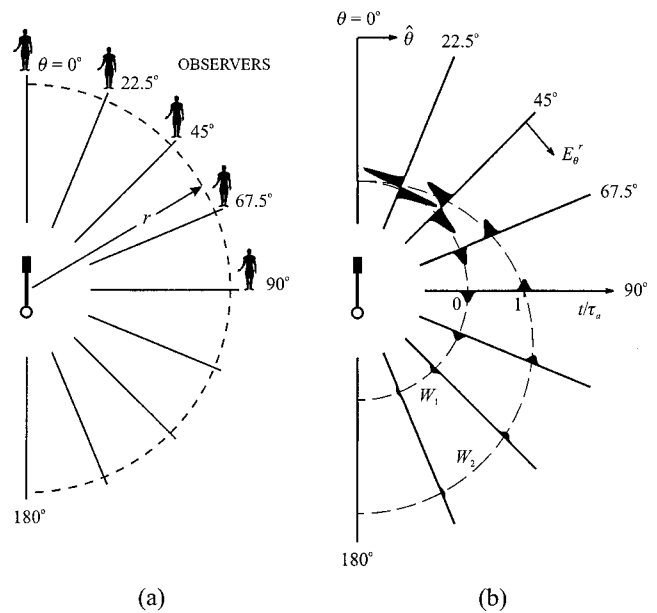


Fig. 5. (a) Schematic drawing showing the observers that record the time-domain wave forms for the radiated field. (b) Radiated or far-zone electric field of the basic traveling-wave element. The excitation is a Gaussian pulse with $\tau/\tau_a=0.076$.

Notice that the separation between the times of arrival for these pulses changes with the angle of observation, θ . This is easily explained with the help of the schematic drawings in Fig. 6. The observer at broadside ($\theta=90^\circ$), shown in Fig. 6(a), receives a signal associated with the pulse of current

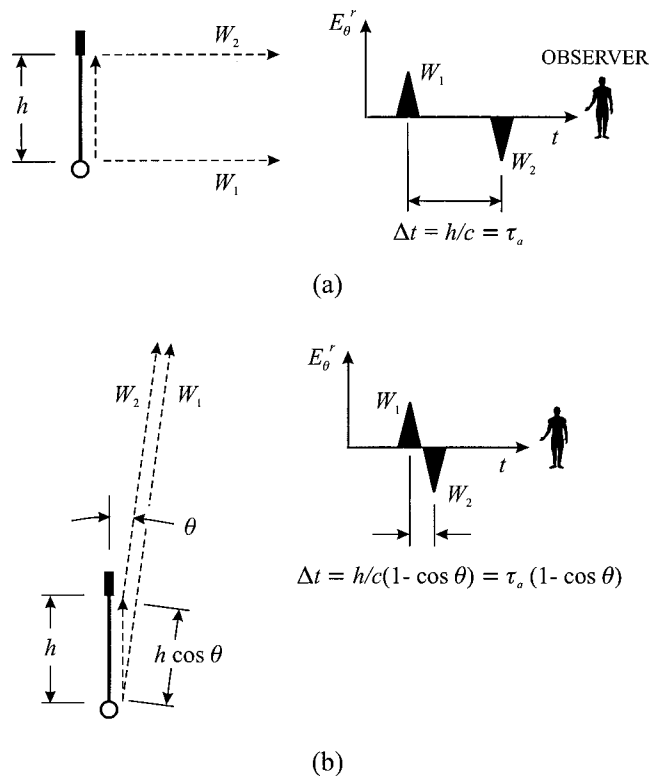


Fig. 6. Schematic drawings used to describe the difference in the times of arrival for the two pulses in the radiated electric field of the basic traveling-wave element.

leaving the source. This is followed by a second signal associated with the pulse of current entering the termination. Both of these signals travel the same distance in free space; however, the pulse of current had to travel an additional distance, h , along the element before reaching the termination. So the two signals are separated in time by $\Delta t = h/c = \tau_a$.

The observer positioned off of the end of the element ($\theta \approx 0^\circ$), shown in Fig. 6(b), receives the two signals at roughly the same time, because the two signals now travel over approximately the same path. When the angle θ is close to zero, the two signals are separated in time by the small amount $\Delta t = \tau_a(1 - \cos \theta) \ll \tau$. The radiated electric field is then approximately proportional to the temporal derivative of the current:

$$\begin{aligned} \mathbf{E}^r(\mathbf{r}, t) &= \frac{\mu_0 h}{4\pi r \Delta t} [I_s(t - r/c) - I_s(t - r/c - \Delta t)] \sin \theta \hat{\theta} \\ &\approx \frac{\mu_0 h}{4\pi r} \frac{dI_s(t - r/c)}{dt} \theta \hat{\theta}. \end{aligned} \quad (15)$$

This is why the field at the angle $\theta = 22.5^\circ$ in Fig. 5(b) resembles the derivative of the Gaussian pulse (14).

An analogy can be drawn between the radiation from this pulse-excited, basic traveling-wave element and the radiation from a moving point charge. When the pulse of charge leaves the source of the element, radiation is produced (a spherical wave front with positive electric field). This is analogous to a point charge undergoing acceleration in the direction of the velocity. As the pulse of charge moves along the element, no radiation is produced. This is analogous to a point charge moving with constant velocity. When the pulse of charge enters the termination of the element, radiation is again produced (a spherical wave front with negative electric field). This is analogous to a point charge undergoing deceleration in the direction of the velocity. Notice that the radiation from the traveling-wave element, shown in Fig. 5(b), is zero in the direction of the motion of the pulse of charge, that is at $\theta = 0^\circ$, and maximum at a small angle to this direction. These characteristics are similar to those for *bremsstrahlung* shown in Fig. 1(b).

III. WIRE ANTENNAS AS SUPERPOSITIONS OF TRAVELING-WAVE ELEMENTS

More complicated wire antennas can be modeled by superimposing basic traveling-wave elements. Before we can perform this superposition, we must obtain the electromagnetic field of a traveling-wave element with a more general orientation than shown in Fig. 3. Consider the orientation shown in Fig. 7. Here, the element is displaced from the z axis so that it lies in the $x-z$ plane with the source end at O' . The translation of the source point is described by the distance d and the angle β ($0 \leq \beta < 2\pi$). In addition, the element is rotated through the angle γ ($0 \leq \gamma < 2\pi$) with respect to the z axis. In the discussion that follows, we will only be concerned with the electromagnetic field at field points, P , that lie in the $x-z$ plane.

The previously obtained formulas for the electromagnetic field, (10) and (11), now apply in the primed coordinate systems ($r', \theta'; r'_h, \theta'_h$) shown in Fig. 7. To use these formulas, we must express these coordinates in terms of the variables

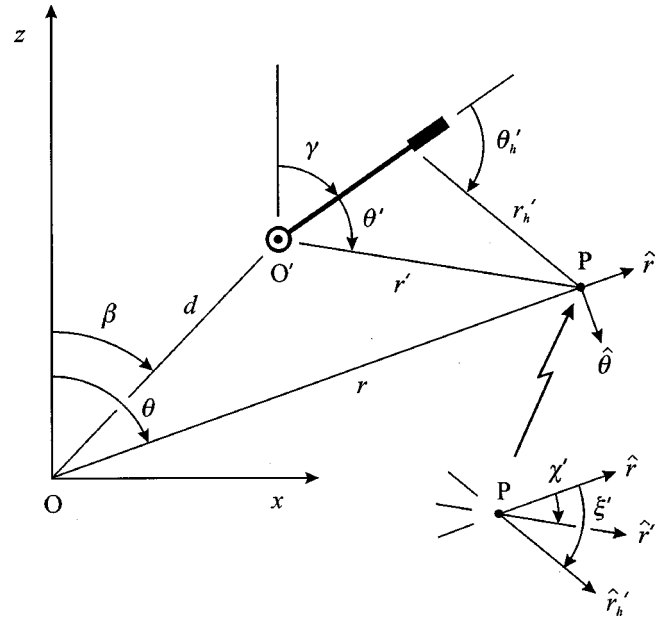


Fig. 7. Coordinates associated with the displaced basic traveling-wave element.

that specify the location and orientation of the element (d, β, γ) and the coordinates of the field point (r, θ):

$$r' = \sqrt{r^2 + d^2 - 2rd \cos(\theta - \beta)}, \quad (16)$$

$$r'_h = \sqrt{(r')^2 + h^2 + 2h[d \cos(\beta - \gamma) - r \cos(\theta - \gamma)]}, \quad (17)$$

$$\cos \theta' = \left[\frac{r \cos(\theta - \gamma) - d \cos(\beta - \gamma)}{r'} \right],$$

$$\sin \theta' = \left[\frac{r \sin(\theta - \gamma) - d \sin(\beta - \gamma)}{r'} \right], \quad (18)$$

$$\cos \theta'_h = \frac{r' \cos \theta' - h}{r'_h}, \quad \sin \theta'_h = \frac{r' \sin \theta'}{r'_h}. \quad (19)$$

The relationships between the unit vectors in the primed and unprimed coordinate systems are

$$\hat{r}' = \cos \chi' \hat{r} + \sin \chi' \hat{\theta}, \quad \hat{\theta}' = -\sin \chi' \hat{r} + \cos \chi' \hat{\theta}, \quad (20)$$

$$\hat{r}'_h = \cos \xi' \hat{r} + \sin \xi' \hat{\theta}, \quad \hat{\theta}'_h = -\sin \xi' \hat{r} + \cos \xi' \hat{\theta}, \quad (21)$$

where the auxiliary angles χ', ξ' , which are shown in the inset in Fig. 7, have been introduced:

$$\chi' = \gamma + \theta' - \theta, \quad \xi' = \gamma + \theta'_h - \theta. \quad (22)$$

Computation of the electromagnetic field of the traveling-wave element using (16)–(22) with (10) and (11) may appear to be a formidable task; however, it is easily accomplished with a simple computer program. For a specified field point (r, θ), first the quantities in (16)–(22) are determined; then, these quantities are substituted into (10) and (11) to determine the field.⁹ For an antenna composed of several basic traveling-wave elements, each with different values of d, β, γ , the field is determined for each element, and the fields of all of the elements are added to obtain the field of the antenna.

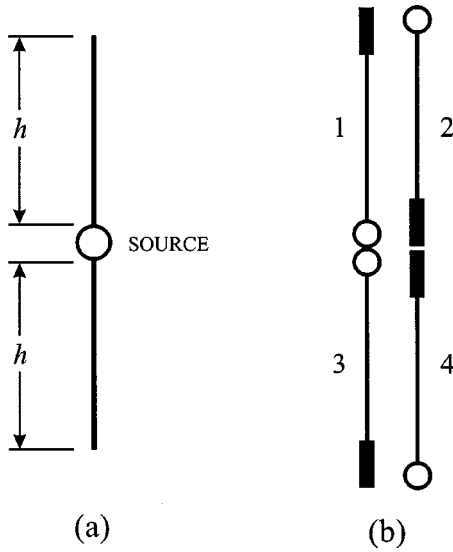


Fig. 8. The standing-wave dipole antenna (a) as a combination of four basic traveling-wave elements (b).

For the special case of the radiated or far-zone field, taking the limit $r/c\tau \rightarrow \infty$ greatly simplifies (16)–(22), so on substitution into (12), we obtain a very simple result for the electric field:

$$\begin{aligned} \mathbf{E}^r(\mathbf{r}, t) = & \frac{\mu_0 c \sin(\theta - \gamma)}{4\pi r [1 - \cos(\theta - \gamma)]} \{ I_s \{ t - [r - d \cos(\theta - \beta)]/c \} \\ & - I_s \{ t - [r - d \cos(\theta - \beta)]/c \\ & - (h/c)[1 - \cos(\theta - \gamma)] \} \} \hat{\theta}. \end{aligned} \quad (23)$$

IV. THE STANDING-WAVE DIPOLE ANTENNA

Our first application of the method of analysis outlined in Sec. III will be to the dipole antenna shown in Fig. 2. We will assume that the source produces a traveling wave of current (a pulse of positive charge) that propagates at the speed of light up the top arm of the dipole. A similar traveling wave of current (a pulse of negative charge) propagates down the bottom arm of the dipole. These waves are totally reflected when they reach the open ends of the dipole at time $t = \tau_a = h/c$. This produces traveling waves of current that propagate on the arms from the open ends toward the source. We will assume that these waves are totally absorbed when they reach the source at time $t = 2\tau_a = 2h/c$.

This dipole antenna can be viewed as the combination of four basic traveling-wave elements shown in Fig. 8. The parameters for each of the elements ($i = 1, 2, 3, 4$) are given in Table I. They are the relative length of the element (h_i/h), the previously defined quantities giving the location and ori-

Table I. Parameters for the four basic traveling-wave elements used to represent the standing-wave dipole antenna.

i	Sign	t_{0i}/τ_a	β_i	d_i/h	γ_i	h_i/h
1	+	0	0	0	0	1
2	+	1	0	1	π	1
3	-	0	0	0	π	1
4	-	1	π	1	0	1

entation of the element ($d_i/h, \beta_i, \gamma_i$), and two new quantities: the “sign” associated with the charge on the element, positive for the top elements and negative for the bottom elements, and the relative time for the excitation of the source of the element (t_{0i}/τ_a). The last quantity accounts for the fact that the sources for all of the elements are not excited at the same time. For example, the excitation of element 2 is delayed by the time $\tau_a = h/c$ from that for element 1 to account for the fact that the pulse has to travel the length of element 1, i.e., h , before it reaches the source end of element 2.

The electromagnetic field of the dipole antenna is the superposition of the electromagnetic fields of the four basic traveling-wave elements:

$$\mathbf{E}(\mathbf{r}, t) = \sum_{i=1}^4 \mathbf{E}_i(\mathbf{r}, t), \quad \mathbf{B}(\mathbf{r}, t) = \sum_{i=1}^4 \mathbf{B}_i(\mathbf{r}, t). \quad (24)$$

To obtain numerical results, this operation can be performed using the formulas presented in Secs. II and III with a simple computer program. However, because the elements are so simply arranged for this example (elements are superimposed and aligned with the z axis), the operation can be performed analytically to give

$$\begin{aligned} \mathbf{E}(\mathbf{r}, t) = & \frac{\mu_0 c}{2\pi r \sin \theta} \{ [I_s(t - r/c) + I_s(t - 2h/c - r/c)] \hat{\theta} \\ & - I_s(t - h/c - r_h/c) \hat{\theta}_h \\ & - I_s(t - h/c - r_{-h}/c) \hat{\theta}_{-h} \}, \end{aligned} \quad (25)$$

$$\begin{aligned} \mathbf{B}(\mathbf{r}, t) = & \frac{\mu_0}{2\pi r \sin \theta} [I_s(t - r/c) + I_s(t - 2h/c - r/c) \\ & - I_s(t - h/c - r_h/c) - I_s(t - h/c - r_{-h}/c)] \hat{\phi}. \end{aligned} \quad (26)$$

There are now three spherical coordinate systems used in the description of the field; they are shown in Fig. 2: the system r, θ, φ with origin at the center of the antenna, the system r_h, θ_h, φ_h with origin at the top of the antenna, and the system $r_{-h}, \theta_{-h}, \varphi_{-h}$ with origin at the bottom of the antenna. The azimuthal coordinate is the same in all systems, so $\hat{\phi}_h = \hat{\phi}_{-h} = \hat{\phi}$. In the limit as $r/c\tau \rightarrow \infty$, (25) simplifies to become the radiated or far-zone electric field:

$$\begin{aligned} \mathbf{E}^r(\mathbf{r}, t) = & \frac{\mu_0 c}{2\pi r \sin \theta} \{ I_s(t - r/c) + I_s(t - r/c - 2h/c) \\ & - I_s[t - r/c - (h/c)(1 - \cos \theta)] \\ & - I_s[t - r/c - (h/c)(1 + \cos \theta)] \} \hat{\theta}. \end{aligned} \quad (27)$$

Figures 9 and 10 show the magnitude of the electric field surrounding the dipole and the radiated electric field, respectively. The parameters and method of construction (times, scaling of the plots, etc.) are the same as used for the graphs for the traveling-wave element in Figs. 4 and 5(b). There are now four spherical wave fronts associated with the radiation. These wave fronts are generated whenever the pulses of current/charge encounter the source or the open ends: W_1 , centered at $z=0$, when the pulses leave the source; W_2 and W_2' , centered at $z=h$ and $z=-h$, respectively, when the pulses are reflected from the open ends; and W_3 , centered at

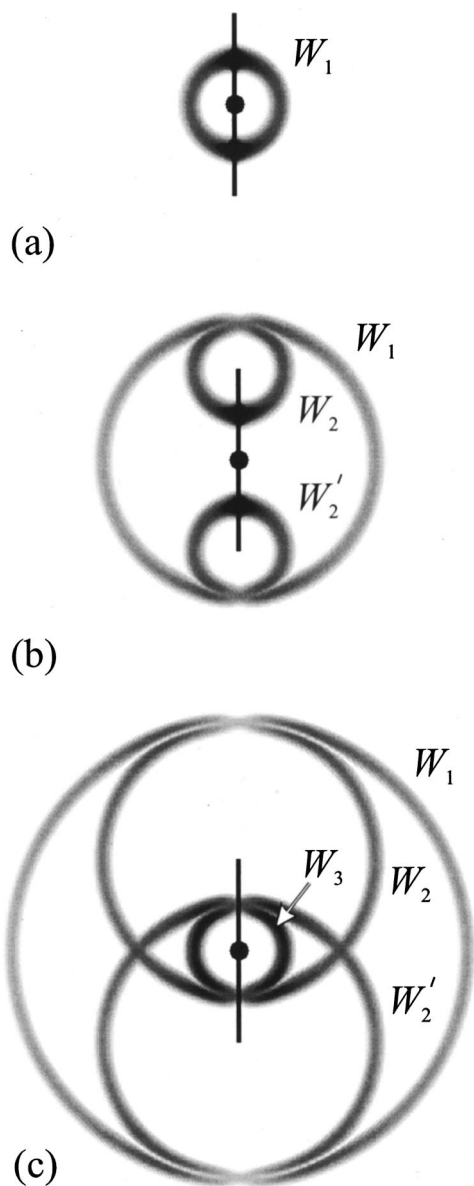


Fig. 9. The magnitude of the electric field surrounding the standing-wave dipole antenna at three times: (a) $t/\tau_a=0.5$, (b) $t/\tau_a=1.5$, and (c) $t/\tau_a=2.5$. The excitation is a Gaussian pulse with $\tau/\tau_a=0.076$.

$z=0$, when the pulses are absorbed at the source. Again, we see the analogy to a moving point charge. Radiation is produced each time the motion of the pulses of current/charge starts, stops, or undergoes a change in direction at the open ends.

Notice that in Fig. 9(c) there is negligible electric field about the source and open ends of the standing-wave dipole. This is to be compared with Fig. 4(c) for the traveling-wave element, where there are strong electric fields about the source and the termination. There is no accumulation of charge at the source or open ends of the dipole; equal amounts of positive and negative charge simultaneously leave or enter the source, and the traveling waves of charge are totally reflected at the open ends.

As discussed in Sec. I, the conventional treatment for the dipole antenna is for time-harmonic excitation. Results for this special case can be obtained using the formulas we have

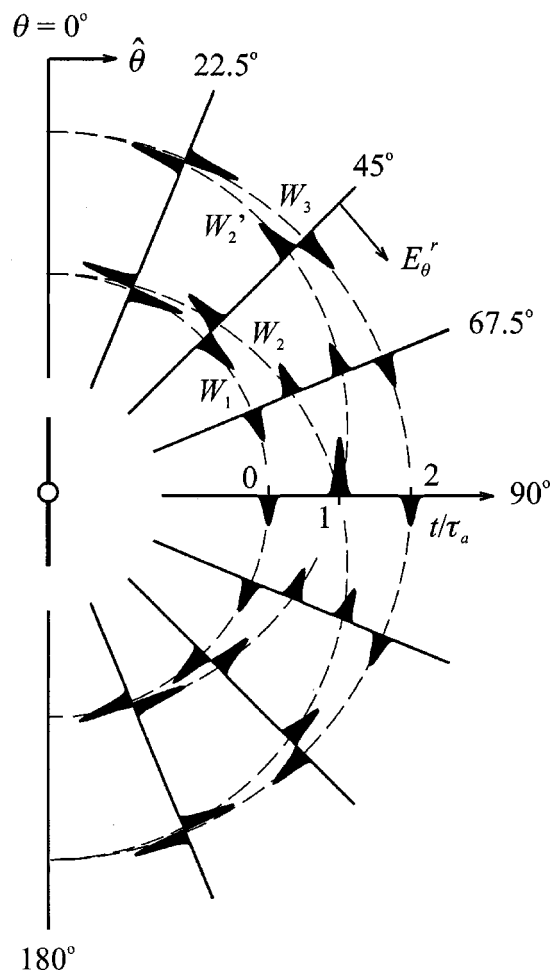


Fig. 10. Radiated or far-zone electric field of the standing-wave dipole antenna. The excitation is a Gaussian pulse with $\tau/\tau_a=0.076$.

presented in this section by simply assuming a time-harmonic current for the source. For example, when we make the current of the source

$$I_s(t) = \text{Re}(I_s e^{j\omega t}), \quad (28)$$

with the phasor

$$I_s = -\frac{j e^{jk_0 h} I_0}{2 \sin(k_0 h)}, \quad (29)$$

and use this current with (27); we obtain the phasor for the radiated electric field given earlier (5).

Figure 11 shows the magnitude of the electric field surrounding the traveling-wave element (a) and the standing-wave dipole (b) for time-harmonic excitation. These graphs were constructed using the expressions for the electromagnetic fields (10) and (25) with a cosinusoidal excitation, instead of the Gaussian pulse used in the earlier examples. These pictures are for a single instant in time and a frequency for which $h/\lambda_0=2$. For this choice of frequency, four half cycles of the cosinusoidal current fit along one element of the antenna. Recall, for the earlier examples, roughly four Gaussian pulses of current fit along one element. Comparing Figs. 11(a) and 11(b) for time-harmonic excitation with Figs. 4 and 9 for pulse excitation, it is clear that the simplicity of the latter makes the interpretation for the origin of the radiation much easier.

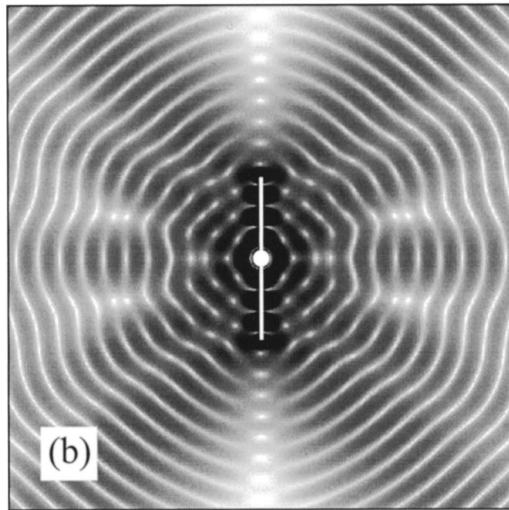
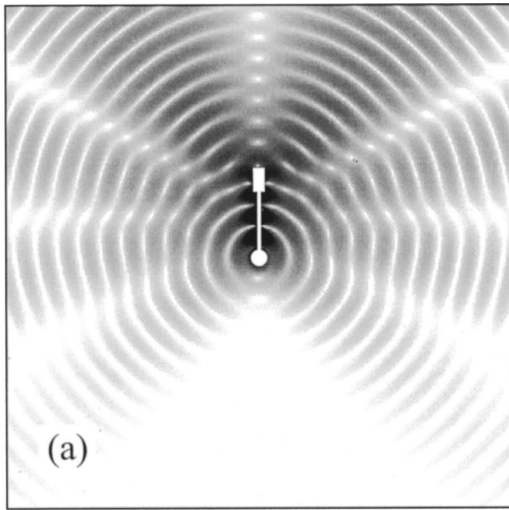


Fig. 11. The magnitude of the electric field surrounding (a) the basic traveling-wave element and (b) the standing-wave dipole antenna for a time-harmonic excitation with $h/\lambda_0 = 2.0$.

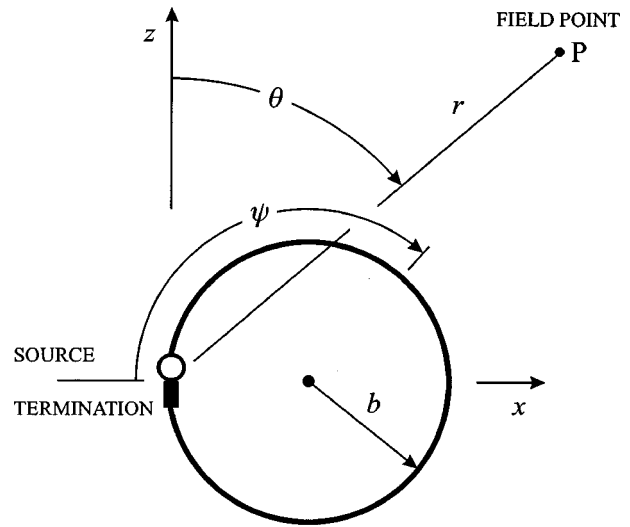
In Fig. 11(a) we can clearly see radial lines on which the magnitude of the electric field is a relative minimum. They are caused by the destructive interference of the electric fields of wave fronts W_1 and W_2 . In between these lines, there are relative maxima caused by constructive interference. Similar behavior is seen in Fig. 11(b).

V. CIRCULAR LOOP ANTENNAS

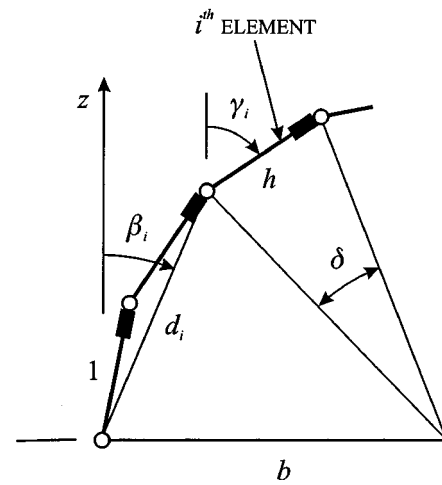
When the wire of an antenna is curved, the antenna can still be viewed as a superposition of basic traveling-wave elements, but the elements are no longer collinear, as they are for the dipole. The curvature of the wire produces additional interesting characteristics for the radiation that we will now examine.

Figure 12(a) shows a traveling-wave, circular loop antenna of radius b . We will assume that the source produces a traveling wave of current (a pulse of positive charge) that propagates at the speed of light in the clockwise direction around the loop until it reaches the termination where it is totally absorbed:¹⁰

$$I_{cw}(\psi, t) = I_s(t - b\psi/c)[U(b\psi) - U(b\psi - 2\pi b)]. \quad (30)$$



(a)



(b)

Fig. 12. (a) Traveling-wave, circular loop antenna. (b) Details for the large number of basic traveling-wave elements used to represent the loop.

The angle ψ ($0 \leq \psi < 2\pi$) in this expression determines the location on the circumference of the loop. This antenna can be viewed as the combination of a large number, $i = 1, 2, 3, \dots, n$, of basic traveling-wave elements. The first few elements in this representation are shown in Fig. 12(b). The parameters that describe these elements are

$$h = 2b \sin(\delta/2), \quad \delta = 2\pi/n, \quad (31)$$

$$d_i = 2b \sin[(i-1)\delta/2], \quad \beta_i = (i-1)\delta/2, \quad (32)$$

$$\gamma_i = (i-1/2)\delta, \quad t_{0i} = \tau_a(i-1)\sin(\delta/2), \quad (33)$$

where $\tau_a = 2b/c$ is now the time for light to travel across the diameter of the loop.

Figure 13 shows the magnitude of the electric field surrounding the loop at two times: $t/\tau_a = 5\pi/8 = 1.96$ and $3\pi/2 = 4.71$, and Fig. 14 shows the radiated or far-zone field. For both plots $\tau/\tau_a = 0.076$, and 65 traveling-wave elements

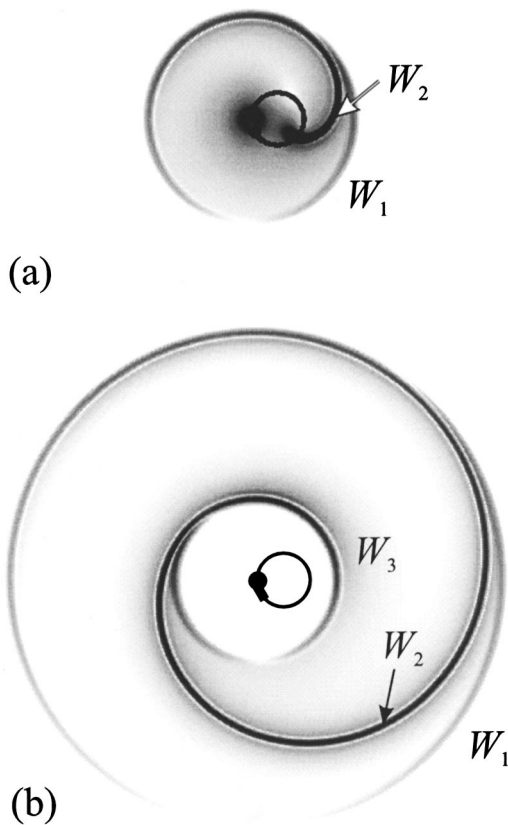


Fig. 13. The magnitude of the electric field surrounding the traveling-wave, circular loop antenna at two times: (a) $t/\tau_a = 5\pi/8 = 1.96$, (b) $t/\tau_a = 3\pi/2 = 4.71$. The excitation is a Gaussian pulse with $\tau/\tau_a = 0.076$.

are used to represent the loop (the length of one element is $h/b = 0.097$). We can distinguish three wave fronts in these figures. The spherical wave fronts W_1 and W_3 are produced when the pulse of current/charge leaves the source and is absorbed at the termination, respectively, and the wave front,

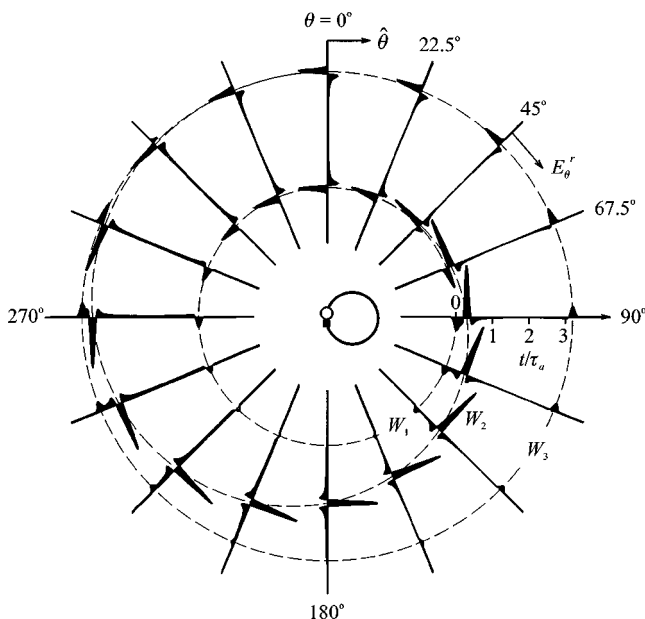


Fig. 14. Radiated or far-zone electric field of the traveling-wave, circular loop antenna. The excitation is a Gaussian pulse with $\tau/\tau_a = 0.076$.

W_2 , is continuously produced as the pulse propagates around the loop. The cause of wave fronts W_1 and W_3 is the same as for the basic traveling-wave element discussed earlier; however, the cause of wave front W_2 is new; it is due to the curvature of the loop.

The schematic drawing in Fig. 15(a) shows the contributions to wave front W_2 from 11 points equally spaced along the loop; it is for the same time as Fig. 13(a), $t/\tau_a = 5\pi/8$. We will use this drawing to explain the spiral shape of this wave front. First we will consider the contribution from point A on the loop. The wave of current/charge leaves the source at point S and travel along the loop until it reaches point A . The path in free space for the radiation from this point onward is tangential to the loop and in the forward direction (in the direction of the motion of the charge). It is shown by the dashed line $A-P$ in Fig. 15(a). The total distance traveled by the signal in going from the source to the point P on W_2 is $d = ct = c(5\pi/8)\tau_a$. This distance is the same for any of the other points shown on the loop. Thus, the longer the distance the signal travels on the loop, the shorter the distance it travels in free space. For the last point, marked B in Fig. 15(a), the signal never leaves the loop; it travels the entire distance d on the loop.

The schematic drawing in Fig. 15(b) shows the details for the radiated electric field at the angle $\theta = 135^\circ$ in Fig. 14. At this angle, the fields of the three wave fronts are clearly separated in time. Wave front W_2 appears to originate at a point on the loop where the tangent line to the loop points in the direction of the observer. As indicated in Fig. 15(b), this can be ascertained from the time of arrival of W_2 relative to W_1 .

Notice that in Fig. 13(a) there is a strong electric field about the source, which is due to the negative charge that remains at the source after the pulse of positive charge leaves. When the pulse of positive charge enters the termination, which is collocated with the source, it cancels this negative charge. Hence, there is negligible electric field around the source and termination in Fig. 13(b).

Recall that for a moving point charge, radiation occurs whenever there is acceleration (1). The acceleration does not have to change the magnitude of the velocity, $|\mathbf{v}|$, or speed to produce radiation—a charge moving over a curved trajectory at constant speed will radiate. For this case, the acceleration is perpendicular to the velocity, and the radiation, shown in Fig. 1(c), is a beam in the direction of the velocity; that is, it is along a line tangent to the trajectory in the direction of the motion. Notice the similarity of this radiation to that for the pulse-excited, curved wire antenna (circular loop). Hence, we can add a new element to the analogy for these two problems: The radiation that occurs as a pulse of current/charge passes along a curved section of a wire antenna is analogous to the *synchrotron* radiation from a point charge traveling at constant speed over a similar curved section of its trajectory.

A standing-wave loop antenna is formed by simply placing a source in a circle of wire [Fig. 12(a) without the termination]. The source produces two traveling waves of current. One is due to a pulse of positive charge propagating in the clockwise direction, as given by Eq. (30), and the other is due to a pulse of negative charge propagating in the counter-clockwise direction:¹¹

$$I_{ccw}(\psi, t) = I_s [t - (2\pi - \psi)b/c] \times [U(b\psi) - U(b\psi - 2\pi b)]. \quad (34)$$

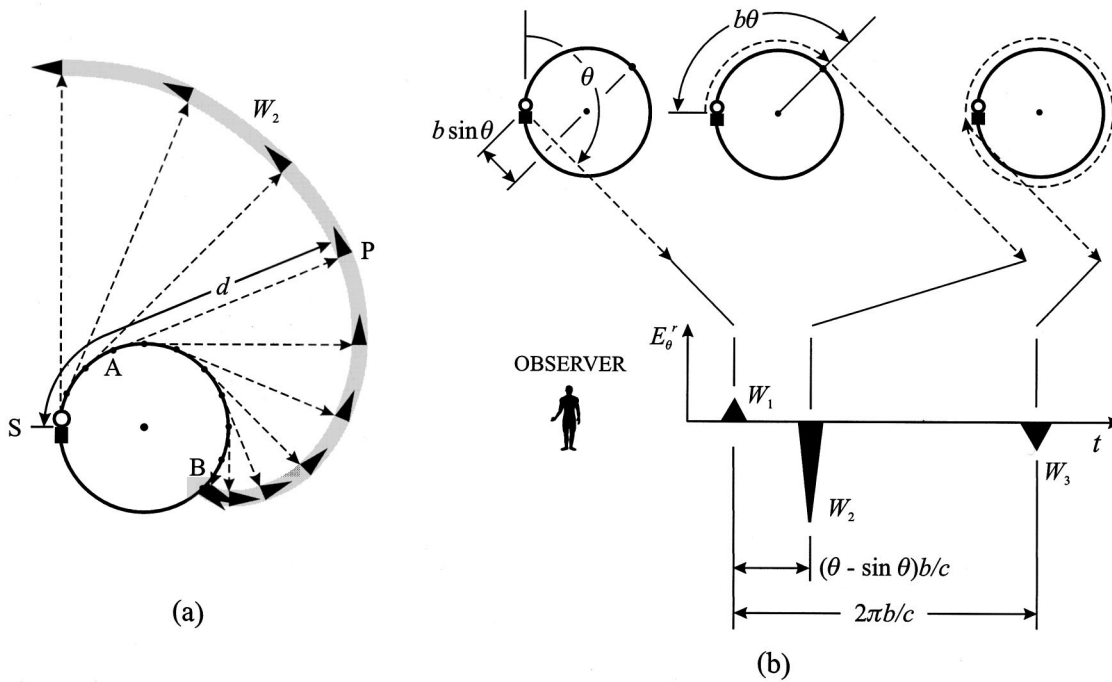


Fig. 15. Schematic drawings used to describe the electric field of the circular, traveling-wave loop antenna. (a) Near field at the time $t/\tau_a = 5\pi/8$. (b) Radiated or far field at the angle $\theta = 3\pi/4 = 135^\circ$.

These waves are partially reflected when they reach the source at time $t = \pi\tau_a = 2\pi b/c$. This produces a new set of traveling waves of current that also propagate around the loop and are partially reflected at the source at time $t = 2\pi\tau_a = 4\pi b/c$. This process is repeated until there is negligible current left on the loop. If we call the reflection coefficient for charge at the source R_Q ($|R_Q| < 1$), the current composed of all of these traveling waves is

$$I(\psi, t) = \sum_{n=0}^{\infty} (-R_Q)^n [I_{cw}(\psi, t - 2\pi n b/c) + I_{ccw}(\psi, t - 2\pi n b/c)], \quad (35)$$

and the electric field of the loop is

$$\mathbf{E}(\mathbf{r}, t) = \sum_{n=0}^{\infty} (-R_Q)^n [\mathbf{E}_{cw}(\mathbf{r}, t - 2\pi n b/c) + \mathbf{E}_{ccw}(\mathbf{r}, t - 2\pi n b/c)], \quad (36)$$

where \mathbf{E}_{cw} is the field of a single clockwise traveling wave of current, and \mathbf{E}_{ccw} is the field of a single counterclockwise traveling wave of current. Each of the fields in this sum can be determined from a superposition of basic traveling-wave elements. When implemented on a computer, the calculation for the total field is only a little more complicated than the calculation for the field of a single traveling wave of current.

The radiated or far-zone electric field for a standing-wave loop antenna with $R_Q = -0.5$ is shown in Fig. 16(a). The other parameters are the same as for the traveling-wave loop antenna discussed earlier. Notice that there are now two symmetrically located, spiral wave forms, W_2 and W_2' ; the former is caused by the clockwise traveling wave of current and the latter by the counterclockwise traveling wave of current.

The thin-wire, circular loop antenna with time-harmonic excitation has been analyzed with a theory based on a Fourier series expansion for the current distribution on the loop.¹² Results from this theory are in excellent agreement with measurements. This theory can be used with the Fourier transform to obtain results for pulse excitation. In Fig. 16(b) we show the radiated field calculated in this manner. For this example, the ratio of the radius of the loop b to the radius of the wire a forming the loop is $b/a = 3500$, and the characteristic impedance of the transmission line feeding the loop is $Z_0 = 100\Omega$. A comparison of these accurate results with those in Fig. 16(a) from our simple, approximate model shows that there is good qualitative agreement. The predictions from the simple model for the location, sense, and relative amplitude of the pulses associated with the various wave fronts are roughly correct.¹³

VI. CONCLUSION

In this paper, a method for obtaining the electromagnetic field of simple wire antennas with a general, assumed distribution of current is presented. The procedure is fairly straightforward: The antenna is viewed as a combination of basic traveling-wave elements, and the electromagnetic field of the antenna is obtained as a superposition of the fields of these elements. An analytic expression is given for the field of the traveling-wave element that can be used in this procedure; it applies at any point in space (near zone or far zone). When the current/charge is a narrow pulse in time, the field at a point in space can be associated with a traveling wave of current passing a particular point on the antenna at an earlier time. Using this observation, a simple analogy is constructed between the radiation from these antennas and the radiation from a moving point charge. This analogy is helpful in predicting the radiation from new, pulse-excited, wire antennas.

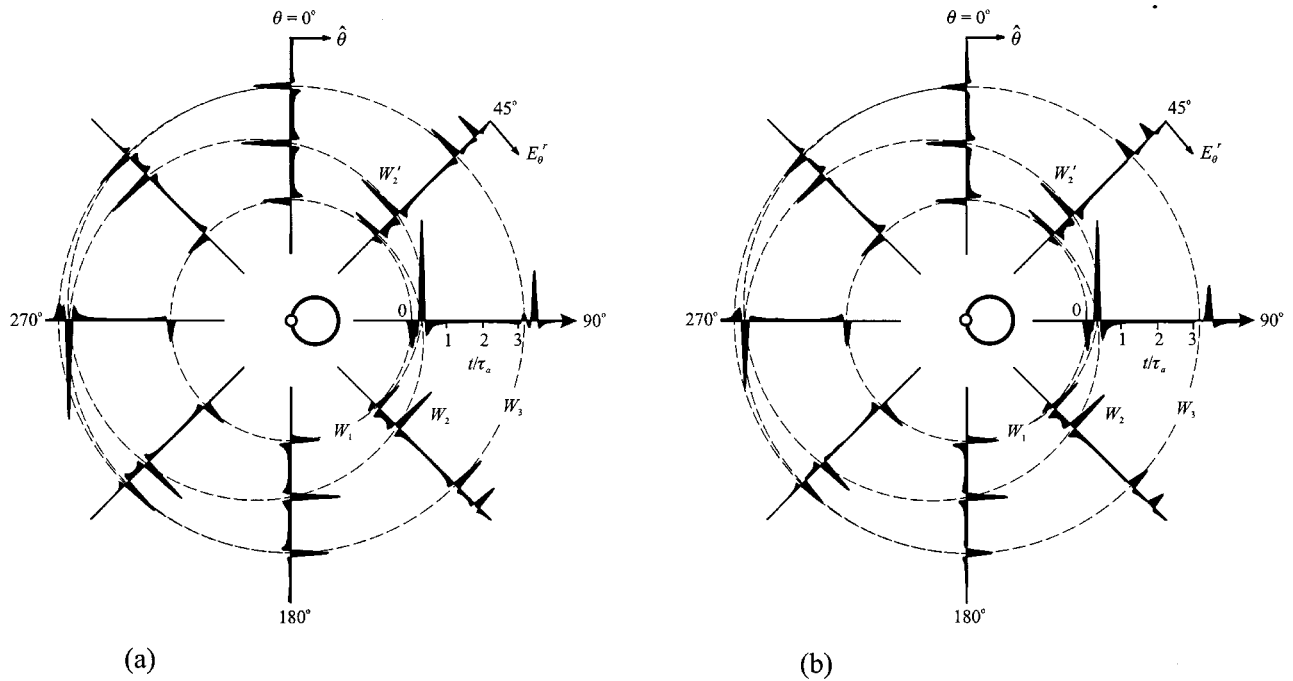


Fig. 16. Radiated or far-zone electric field of the standing-wave, circular loop antenna. The excitation is a Gaussian pulse with $\tau/\tau_a=0.076$. (a) Computed using a superposition of basic traveling-wave elements, $R_0=-0.5$. (b) Computed using an accurate analysis based on a Fourier series expansion for the current, $b/a=3500$, $Z_0=100\Omega$.

The analogy with the moving point charge can be extended to include phenomena not discussed in this paper. As an example, we mention the pulse-excited, insulated, linear antenna. This is a wire antenna coated with a concentric, cylindrical, dielectric sheath and placed in a medium with a permittivity that is higher than that of the sheath. In a practical application, the sheath could be plastic, and the surrounding medium could be soil or water. Because of the difference in the permittivities of the sheath and the surrounding medium, the wave of current/charge on this antenna travels at a speed greater than the speed of light in the surrounding medium. This produces radiation that is analogous to Cherenkov radiation, which occurs whenever the speed of a moving point charge is greater than the speed of light in the surrounding medium.¹⁴

Models like the one presented in this paper, whether they are for pulse excitation or for time-harmonic excitation, have a common weakness—they are based on an assumed, approximate current distribution on the antenna. The electromagnetic fields calculated from these models are generally in good qualitative agreement with more accurate predictions and measurements, and they are generally sufficient for understanding the physical phenomena associated with the radiation. However, these models cannot be relied upon for precise calculations of other quantities, such as the input impedance of the antenna, that are more sensitive to the form of the current.

The methodology presented in this paper is for transmitting antennas; a similar methodology has been developed for receiving antennas. Perhaps the receiving antenna will be the subject of a future paper.

ACKNOWLEDGMENTS

The author would like to thank Dr. Guangping Zhou for providing the data for the graph in Fig. 16(b). The author is

grateful for the support provided by the John Pippin Chair in Electromagnetics that furthered this study. This research was supported in part by the Army Research Office under Contract No. DAAG55-98-1-0403.

APPENDIX A: CHARGE PER UNIT LENGTH ON THE BASIC TRAVELING-WAVE ELEMENT

The equation of continuity for electric charge in one spatial dimension,

$$\frac{\partial I(z,t)}{\partial z} = -\frac{\partial Q(z,t)}{\partial t}, \quad (\text{A1})$$

can be integrated to give

$$Q(z,t) = -\int_{t'=-\infty}^t \frac{\partial I(z,t')}{\partial z} dt', \quad (\text{A2})$$

where it is assumed that $Q(z,t=-\infty)=0$. On substitution of the distribution of current (7), (A2) becomes

$$\begin{aligned} Q(z,t) &= -\int_{t'=-\infty}^t \frac{\partial I_s(t'-z/c)}{\partial z} dt' [U(z) - U(z-h)] \\ &\quad - \int_{t'=-\infty}^t I_s(t'-z/c) dt' \frac{\partial}{\partial z} [U(z) - U(z-h)] \\ &= -\int_{t'=-\infty}^t \frac{\partial I_s(t'-z/c)}{\partial z} dt' [U(z) - U(z-h)] \\ &\quad - \int_{t'=-\infty}^t I_s(t') dt' \delta(z) \\ &\quad + \int_{t'=-\infty}^t I_s(t'-h/c) dt' \delta(z-h). \end{aligned} \quad (\text{A3})$$

Now we can use the relation

$$\frac{\partial I_s(t-z/c)}{\partial z} = -\frac{1}{c} \frac{\partial I_s(t-z/c)}{\partial t} \quad (\text{A4})$$

to evaluate the first integral and obtain the final expression for the charge per unit length:

$$\begin{aligned} Q(z,t) = & \frac{1}{c} I_s(t-z/c) [U(z) - U(z-h)] \\ & - \int_{t'=-\infty}^t I_s(t') dt' \delta(z) + \int_{t'=-\infty}^t I_s(t'-h/c) \\ & \times dt' \delta(z-h), \end{aligned} \quad (\text{A5})$$

where it is assumed that $I_s(z,t=-\infty)=0$. After using the notation given in (9), (A5) becomes (8).

APPENDIX B: ELECTROMAGNETIC FIELD OF THE BASIC TRAVELING-WAVE ELEMENT

The scalar electric potential Φ and the vector magnetic potential \mathbf{A} in the Lorentz gauge are given by the following integrals of the volume charge density ρ and volume current density \mathbf{J} :

$$\begin{aligned} \Phi(\mathbf{r},t) = & \frac{1}{\epsilon_0} \int_{t'=-\infty}^{\infty} \int \int \int_V \rho(\mathbf{r}',t') \\ & \times G_0(\mathbf{r},\mathbf{r}';t,t') dV' dt', \end{aligned} \quad (\text{B1})$$

$$\begin{aligned} \mathbf{A}(\mathbf{r},t) = & \mu_0 \int_{t'=-\infty}^{\infty} \int \int \int_V \mathbf{J}(\mathbf{r}',t') \\ & \times G_0(\mathbf{r},\mathbf{r}';t,t') dV' dt', \end{aligned} \quad (\text{B2})$$

where \mathbf{r}' locates the source point, \mathbf{r} locates the field point, and G_0 is the free-space, scalar Green's function:¹⁵

$$G_0(\mathbf{r},\mathbf{r}';t,t') = \frac{\delta(t-t'-R/c)}{4\pi R}, \quad R = |\mathbf{r}-\mathbf{r}'|. \quad (\text{B3})$$

For the basic traveling-wave element, the charge and current are confined to the z axis, and there is only one component to the current (z); hence, (B1) and (B2) simplify to become

$$\begin{aligned} \Phi(\mathbf{r},t) = & \frac{1}{\epsilon_0} \int_{t'=-\infty}^{\infty} \int_{z'=-\infty}^{\infty} Q(z',t') \\ & \times G_0(\mathbf{r},z';t,t') dz' dt', \end{aligned} \quad (\text{B4})$$

$$\begin{aligned} A_z(\mathbf{r},t) = & \mu_0 \int_{t'=-\infty}^{\infty} \int_{z'=-\infty}^{\infty} I(z',t') \\ & \times G_0(\mathbf{r},z';t,t') dz' dt', \end{aligned} \quad (\text{B5})$$

with

$$\begin{aligned} G_0(\mathbf{r},z';t,t') = & \frac{\delta(t-t'-R/c)}{4\pi R}, \\ R = & \sqrt{x^2+y^2+(z-z')^2}. \end{aligned} \quad (\text{B6})$$

After inserting the charge (8) into (B4) and the current (7) into (B5), using the properties of the step and delta functions, and introducing the change of variable

$$\eta = t - R/c - z'/c, \quad d\eta = \frac{\eta + z/c - t}{R} dz', \quad (\text{B7})$$

the potentials become

$$\begin{aligned} \Phi(\mathbf{r},t) = & \frac{1}{4\pi\epsilon_0} \left[\frac{1}{r} q_0(t-r/c) + \frac{1}{r_h} q_h(t-r_h/c) \right. \\ & \left. + \int_{\eta=t-r/c}^{t-h/c-r_h/c} \frac{Q_s(\eta)}{\eta+z/c-t} d\eta \right], \end{aligned} \quad (\text{B8})$$

$$A_z(\mathbf{r},t) = \frac{\mu_0}{4\pi} \int_{\eta=t-r/c}^{t-h/c-r_h/c} \frac{I_s(\eta)}{\eta+z/c-t} d\eta. \quad (\text{B9})$$

Now the potential functions must be differentiated to obtain the electric and magnetic fields:

$$\mathbf{E} = -\nabla\Phi - \frac{\partial A_z}{\partial t} \hat{z}, \quad (\text{B10})$$

$$\mathbf{B} = \nabla \times (A_z \hat{z}) = -\hat{z} \times \nabla A_z. \quad (\text{B11})$$

After inserting (B8) and (B9) into (B10) and (B11) and using Leibniz's rule to differentiate the integrals, the electric and magnetic fields become

$$\begin{aligned} \mathbf{E}(\mathbf{r},t) = & -\frac{1}{4\pi\epsilon_0} \left\{ \nabla \left[\frac{q_0(t-r/c)}{r} \right] + \nabla_h \left[\frac{q_h(t-r_h/c)}{r_h} \right] \right. \\ & - \left[\frac{I_s(t-r/c)}{z-r} \right] \nabla(t-r/c) \\ & + \left[\frac{I_s(t-h/c-r_h/c)}{(z-h)-r_h} \right] \nabla_h(t-h/c-r_h/c) \\ & + \int_{\eta=t-r/c}^{t-h/c-r_h/c} \frac{1}{c} I_s(\eta) \nabla \left(\frac{1}{\eta+z/c-t} \right) d\eta \\ & - \frac{1}{c} \left[\frac{I_s(t-r/c)}{z-r} - \frac{I_s(t-h/c-r_h/c)}{(z-h)-r_h} \right] \\ & \left. - \int_{\eta=t-r/c}^{t-h/c-r_h/c} \frac{1}{c} I_s(\eta) \frac{\partial}{\partial t} \left(\frac{1}{\eta+z/c-t} \right) d\eta \right\} \hat{z}, \end{aligned} \quad (\text{B12})$$

$$\begin{aligned} \mathbf{B}(\mathbf{r},t) = & \hat{z} \times \left\{ \frac{\mu_0}{4\pi} \left\{ c \left[\frac{I_s(t-r/c)}{z-r} \right] \nabla(t-r/c) \right. \right. \\ & - c \left[\frac{I_s(t-h/c-r_h/c)}{(z-h)-r_h} \right] \nabla_h(t-h/c-r_h/c) \\ & \left. \left. - \int_{\eta=t-r/c}^{t-h/c-r_h/c} I_s(\eta) \nabla \left(\frac{1}{\eta+z/c-t} \right) d\eta \right\} \right\}. \end{aligned} \quad (\text{B13})$$

It is permissible to perform the gradient and curl operation in (B10) and (B11) in either of the two spherical coordinate systems shown in Fig. 3. Thus, in (B12) and (B13) we have ∇ when the coordinates r, θ, φ are to be used and ∇_h when the coordinates r_h, θ_h, φ_h are to be used. Now the final expressions for the electric and magnetic fields are obtained by performing the differentiations in (B12) and (B13) and combining terms:

$$\mathbf{E}(\mathbf{r}, t) = \frac{1}{4\pi\epsilon_0} \left[\frac{q_0(t-r/c)}{r^2} \hat{\mathbf{r}} + \frac{q_h(t-r_h/c)}{r_h^2} \hat{\mathbf{r}}_h + \frac{\cot(\theta/2)I_s(t-r/c)}{cr} \hat{\boldsymbol{\theta}} - \frac{\cot(\theta_h/2)I_s(t-h/c-r_h/c)}{cr_h} \hat{\boldsymbol{\theta}}_h \right], \quad (\text{B14})$$

$$\mathbf{B}(\mathbf{r}, t) = \frac{\mu_0}{4\pi} \left[\frac{\cot(\theta/2)I_s(t-r/c)}{r} - \frac{\cot(\theta_h/2)I_s(t-h/c-r_h/c)}{r_h} \right] \hat{\boldsymbol{\phi}}. \quad (\text{B15})$$

¹G. S. Smith, *An Introduction to Classical Electromagnetic Radiation* (Cambridge U.P., Cambridge, 1997), Chap. 6, Sec. 6.1.2, pp. 364–371.

²Some of the textbooks that follow this approach are: J. B. Marion and M. A. Heald, *Classical Electromagnetic Radiation* (Academic, New York, 1980), 2nd ed., pp. 247–257; J. R. Reitz, F. J. Milford, and R. W. Christy, *Foundations of Electromagnetic Theory* (Addison–Wesley, Reading, MA, 1993), 3rd ed., pp. 529–531; J. Schwinger, L. L. DeRaad, Jr., K. A. Milton, and W. Tsai, *Classical Electrodynamics* (Perseus, Reading, MA, 1998), pp. 367–374; J. D. Jackson, *Classical Electrodynamics* (Wiley, New York, 1999), 3rd ed., pp. 416–417.

³The superscript r is used to indicate the radiated field.

⁴See Ref. 1, Chap. 8, pp. 546–607; G. S. Smith, “On the interpretation for radiation from simple current distributions,” *IEEE Antennas and Propagat. Mag.* **40**, 39–44 (August 1998).

⁵This is actually the current distribution for a section of ideal transmission line of length h terminated with a reflectionless load. Here we are assuming the current on the antenna is similar to that on the transmission line. This assumption is good whenever the wire forming the antenna is infinitesimally thin, see for example, S. A. Schelkunoff, *Advanced Antenna Theory* (Wiley, New York, 1952), pp. 102–110; A. Sommerfeld, *Electrodynamics* (Academic, New York, 1952), pp. 177–186.

⁶There is a long history associated with the derivation and physical interpretation of formulas similar to the ones presented here for the electromagnetic field of an assumed filamentary current distribution. In 1899 Heaviside discussed the reflection of an impulsive electromagnetic wave at the free ends of a wire and made sketches of the electromagnetic field surrounding the wire that are similar to those in Fig. 9: O. Heaviside, *Electromagnetic Theory* (The Electrician Printing and Publishing Co., London, 1899; Republication, Chelsea, New York, 1971), Vol. II, pp. 367–372. In 1923 Manneback analyzed the radiation from a parallel-wire transmission line: C. Manneback, “Radiation from transmission lines,” *J. Am. Inst. Electr. Eng.* **42**, 95–105 (1923); **42**, 981–982 (1923); **42**, 1362–1365 (1923). And later Schelkunoff extended Manneback’s treatment and applied it to thin-wire antennas; S. A. Schelkunoff, *Advanced Antenna Theory* (Wiley, New York, 1952), pp. 102–109. More recently, formulas similar to those presented here for the electromagnetic field have been

obtained by a number of authors. The reader is cautioned that some of the earlier papers contain errors and inconsistencies that are pointed out in the later papers. Z. Q. Chen, “Theoretical solutions of transient radiation from traveling-wave linear antennas,” *IEEE Trans. Electromagn. Compat.* **30**, 80–83 (1988); J. Zhan and Q. L. Qin, “Analytic solutions of traveling-wave antennas excited by nonsinusoidal currents,” *ibid.* **31**, 328–330 (1989); L. Fang and W. Wenbing, “An analysis of the transient fields of linear antennas,” *ibid.* **31**, 404–409 (1989); E. J. Rothwell and M. J. Cloud, “Transient field produced by a traveling-wave wire antenna,” *ibid.* **33**, 172–178 (1991); S. A. Podosenov, Y. G. Svekis, and A. A. Sokolov, “Transient radiation of traveling waves by wire antennas,” *ibid.* **37**, 367–383 (1995); G. Wang and W. B. Wang, “Comments on transient radiation of traveling waves by wire antennas,” *ibid.* **39**, 265 (1997); D. Wu and C. Ruan, “Transient radiation of traveling-wave wire antennas,” *ibid.* **41**, 120–123 (1999). Results for the radiated field or far-zone field are given in several places, for example, D. L. Sengupta and C.-T. Tai, “Radiation and reception of transients by linear antennas,” in *Transient Electromagnetic Fields*, edited by L. B. Felsen (Springer, New York, 1976), Chap. 4; R. G. Martin, J. A. Morente, and A. R. Bretones, “An approximate analysis of transient radiation from linear antennas,” *Int. J. Electron.* **61**, 343–353 (1986).

⁷The electric field at the element is infinite. Thus, for these plots, the field must be clipped when it is above a reference value $|\mathbf{E}|_{\max}$. When the Gaussian pulse is out along the element, the peak value of the electric field (in time) in the region of the element containing the pulse is $|\mathbf{E}| \approx \mu_0 c I_0 / 2\pi\rho$, where ρ is the radial distance from the element. This relation can be used to choose a value for $|\mathbf{E}|_{\max}$.

⁸In this graph and in similar graphs that follow, the electric field for each plot is positive in the clockwise direction measured from the time axis. For the time axis at the angle $\theta=45^\circ$ in Fig. 5(b), this direction is indicated by an arrow.

⁹For the numerical evaluation of (10) and (11), it is sometimes useful to make the substitution $\cot(x/2) = \sin x / (1 - \cos x) = (1 + \cos x) / \sin x$.

¹⁰Here, we are assuming that the wave is not reflected as it travels along the loop, and that there is no accumulation of charge on the loop.

¹¹Current is taken to be positive when it is in the direction of increasing ψ . Thus, a pulse of positive charge traveling in the clockwise direction is a positive current (30), and a pulse of negative charge traveling in the counterclockwise direction is also a positive current (34).

¹²R. W. P. King and G. S. Smith, *Antennas in Matter: Fundamentals, Theory, and Applications* (MIT, Cambridge, MA, 1981), Chap. 9, pp. 527–570; G. Zhou and G. S. Smith, “An accurate theoretical model for the thin-wire circular half-loop antenna,” *IEEE Trans. Antennas Propag.* **39**, 1167–1177 (1991).

¹³The good agreement is partly the result of choosing the wire of the loop to be very thin. For thicker wire, there will be noticeable differences; for example, for the actual antenna, the pulses will decrease in amplitude more rapidly with increasing t/τ_a than for the simple model.

¹⁴See Ref. 1, pp. 579–583; T. W. Hertel and G. S. Smith, “Pulse radiation from an insulated antenna: An analog of Cherenkov radiation from a moving charged particle,” *IEEE Trans. Antennas Propag.* **48**, 165–172 (2000).

¹⁵See Ref. 1, pp. 341–347.

TOO MANY PEARLS?

Newton, in a scholium to his Third Law of Motion, has stated the relation between work and kinetic energy in a manner so perfect that it cannot be improved, but at the same time with so little apparent effort or desire to attract attention that no one seems to have been struck with the great importance of the passage till it was pointed out recently by Thomson and Tait.

James Clerk Maxwell, *Theory of Heat* (Appleton, New York, 1872), p. 91.